



Mini Review of Glucose Detection Using Plasmonic Sensor

Natasya Salsabiila^{1,2}, Marlia Morsin^{1,2*}, Suratun Nafisah³, Nur Liyana Razali^{1,2}, Farhanani Mahmud^{1,2}, Zarina Tukiran^{1,2,4}

¹Faculty of Electrical and Electronic Engineering,
Universiti Tun Hussein Onn Malaysia, 86400 Parit Raja, Batu Pahat, Johor, MALAYSIA

²Microelectronics and Nanotechnology – Shamsuddin Research Centre, Institute of Integrated Engineering,
Universiti Tun Hussein Onn Malaysia, 86400 Parit Raja, Batu Pahat, Johor, MALAYSIA

³Department of Electrical Engineering,
Institut Teknologi Sumatera, 35365 Jln. Terusan Ryacudu, Way Hui, Jatiagung, Lampung Selatan, INDONESIA

⁴Internet of Things Focus Group, Faculty of Electrical and Electronic Engineering,
Universiti Tun Hussein Onn Malaysia, 86400 Parit Raja, Batu Pahat, Johor, MALAYSIA

*Corresponding Author

DOI: <https://doi.org/10.30880/emait.2023.04.01.006>

Received 2 March 2023; Accepted 19 June 2023; Available online 28 June 2023

Abstract: Glucose is a crucial compound in human life. Glucose has important roles in energy source production and overall brain health. In addition, it can be converted into other compounds essential for the growth, repair, and maintaining tissues throughout the body. Also, glucose becomes an indicator of diabetes, i.e., ill when the body can not produce insulin hormone properly. The poor management of diabetes can affect long-term complications that can significantly impact a person's quality of life and may lead to disability or even premature death if not properly addressed. Thus, it is important to do glucose detection to stay within a healthy range. The common methods patients use are glucose meters and urine testing on the laboratory scale. This method has several areas for improvement, such as being invasive, needing experts, and requiring a long-time detection. Thus, researchers come into various alternative glucose detection such as chromatography, mass spectrometry, electrochemical, and plasmonic sensor. Chromatography for glucose detection is rarely used in recent years because of its complexity. Then, for mass spectrometry, it is also complicated for the result and maintenance. As for electrochemical methods, the disadvantage is that other electroactive components on the sample can be interfered with. Plasmonic sensors that utilize the Localized Surface Plasmon Resonance (LSPR) phenomenon are considered due to their advantage, i.e., non-invasive, real-time monitoring, and highly sensitive to surrounding medium change. Plasmonic sensors usually use components of light absorption, luminescence, fluorescence, Raman scattering, reflectance, and refractive index based on the nanoparticles used as sensing materials. Still, transmission and reflection are popular and widely applied. Furthermore, plasmonic sensors generally consist of instruments such as a light source, fiber optic, chamber to place substrate/analyte, spectrometer/detector, and computer. Besides, plasmonic sensors can produce different analytical characteristics suitable for different cases and tuned for the need because of the various sensing materials used. Hence, plasmonic sensors become a promising alternative method for glucose detection.

Keywords: Localized surface plasmon resonance, glucose detection, plasmonic sensor

1. Introduction

Glucose plays a crucial role in human life as it is the primary energy source for the body's cells and is involved in various physiological processes. Besides playing a role in energy production through the formation of adenosine

triphosphate (ATP) [1], glucose is crucial for maintaining cognitive function, memory, and overall brain health because the brain is an organ that does not depend on alternative fuels [2]. Also, glucose is a central player in various metabolic processes. It can be converted into other molecules to synthesize essential compounds, including lipids (fats), proteins, and nucleic acids (DNA and RNA). These processes are essential for growth, repair, and maintaining tissues throughout the body [3]. The important role of glucose is to become an indicator of diabetes, the kind of ill that the body either does not produce enough insulin or does not effectively use it [4]. Poorly managed diabetes can lead to various complications that affect different organs and systems in the body. Long-term complications include cardiovascular disease, nerve damage (neuropathy), kidney damage (nephropathy), eye damage (retinopathy), foot ulcers, and an increased risk of infections. These complications can significantly impact a person's quality of life and may lead to disability or even premature death if not properly addressed [5]–[7]. Thus, detecting glucose in the human body is important so levels are still within normal limits.

The times have led to the development of glucose detection methods. The conventional methods of glucose detection are using glucose meters and urine testing. The disadvantage of this method is invasive, so it causes damage to human tissue, is performed by experts, and requires a long-time detection within 2 hours [8], [9]. Therefore, several advance methods have been developed for glucose detection, such as chromatographic, mass spectrometry, electrochemical, and plasmonic sensor. A plasmonic sensor that utilizes the optical phenomenon called Localized Surface Plasmon Resonance, which generates from the nanoparticles as the sensing materials, is often preferred for glucose detection. These techniques provide the potential for real-time glucose monitoring and are painless and non-invasive for the patients. Therefore, it is possible to detect glucose levels constantly or regularly, giving current data on glucose swings. To properly manage diabetes, real-time monitoring is important because it enables prompt modifications to food, insulin doses, and other lifestyle variables depending on glucose levels [10]. Additionally, since plasmonic sensors are extremely sensitive, they may pick up even minute changes in the refractive index of the medium around them. This qualifies them to detect glucose levels in body fluids like urine or saliva [11]. Hence, this work reviews plasmonic sensors as an alternative glucose detection method using various nanoparticles as the sensing materials.

2. Glucose

Because it serves as the main energy source for most organisms, glucose is one of the most important biological substances in existence. The kind of sugar known as glucose is metabolized by cells as part of cellular respiration to create adenosine triphosphate (ATP), which is then utilized by cells for various processes, including muscular contraction, nerve impulse transmission, and protein synthesis. Additionally, glucose is essential since it is the brain's main fuel supply. Furthermore, glucose may be transformed into other crucial biomolecules, including glycogen, which is stored in the liver and muscles and utilized as energy, as well as several amino acids required to construct proteins [1].

Diabetes is frequently diagnosed using glucose levels. Diabetes causes high blood glucose levels because the body struggles to control blood glucose levels. Glucose monitoring is essential for people with diabetes to keep blood sugar levels within a reasonable range [12]. Diabetes impairs the body's capacity to control glucose, which causes substantial fluctuations in blood glucose levels. As a result, blood glucose levels may rise too much, which can cause some health issues, including cardiovascular disease, nerve damage, and renal damage [13].

2.1 Chemical and Physical Properties of Glucose

Glucose has a monosaccharide molecular structure with the following formula: $C_6H_{12}O_6$. In this structure, the six carbon atoms are numbered from 1 to 6, and the hydroxyl (-OH) groups are attached to each carbon atom, except for one that has an aldehyde (-CHO) group instead [14]. The chemical structure of glucose is shown in Fig. 1. Then, the properties of glucose are shown in Table 1.

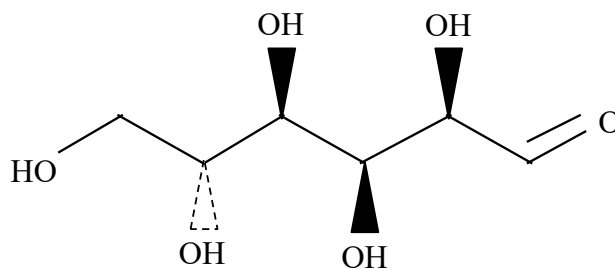


Fig. 1 - Chemical structure of glucose

Table 1 - Chemical and physical properties of glucose

Property name	Property value	Remarks
Molecular weight	180.16 g/mol	-
Density	1.54 g/cm ³	-
Melting point	146 – 150 °C	-
Boiling point	553.5°C	-
Optical rotation	+52.5°	-
pH	Slightly acidic	pKa = 12.2 and 14 for two hydroxyl groups
Solubility	Water, ethanol, and methanol	Insoluble in non-polar solvents
Reactivity	Oxidation, glycosylation, and mutarotation	-

2.2 Glucose in The Human Body

Usually, glucose concentration in the human bloodstream is 3.8 –6.9 mM in an empty stomach and 3.9 – 7.8 mM after food. A level below 2.8 mM after no eating or the following exercise is considered hypoglycemia. For people with diabetes, the blood glucose concentration should be strictly controlled below 10 mM, according to the American Diabetes Association [15]. Meanwhile, using mg/dL unit, in the condition before eating, the standard blood sugar content is 70 – 130 mg/dl. Then in the situation 2 h after eating, regular blood sugar content is < 140 mg/dl. For fasting conditions for at least 8 h, the standard blood sugar content is < 100 mg/dl. Meanwhile, for bedtime conditions, normal blood sugar levels are 100 – 140 mg/dl [16].

There are 3 primary types of diabetes, i.e., type 1, type 2, and gestational. Type 1 diabetes is an autoimmune disease in which the immune system attacks and destroys insulin-producing cells in the pancreas. This type of diabetes is usually diagnosed in children and young adults [17]. Then type 2 diabetes is a metabolic disorder in which the body cannot use insulin effectively, resulting in high blood sugar levels. It is often associated with obesity and a sedentary lifestyle and can be managed with lifestyle changes and medication [18]. On the other hand, gestational diabetes manifests throughout pregnancy and commonly goes away after birth. Nevertheless, type 2 diabetes is more likely to develop in women with gestational diabetes [19].

3. Detection Methods for Glucose

A glucose meter, which uses the enzyme glucose oxidase to quantify the quantity of glucose in a tiny blood sample, is the common method of determining blood glucose levels. Typically, a lancet is used to nick the finger, a drop of blood is placed on a test strip, and the strip is placed into a glucose meter to get the blood sample [20]. Additionally, glucose might be discovered in urine samples. Although the quantities of glucose in the blood and urine are usually different, glucose in the urine can still be a sign of diabetes or other conditions [21]. Using glucose test strips containing the enzyme glucose oxidase is the most common way to determine whether there is glucose in urine. The quantity of glucose in the urine samples may then be calculated by comparing the intensity of the color shift to a color chart. However, it should be noted that urine glucose levels can be affected by factors such as hydration, exercise, and medication [22].

Now, several advance methods are used to determine glucose in human blood. Chromatographic, mass spectrometry, electrochemical, and plasmonic sensor are developed to detect glucose. The research by Wei-qi et al. used reaction headspace in gas chromatography to detect glucose [23]. Gas chromatography is also used in the research by Paulin et al., with methyloxime peracetate derivatized aldose and ketose as fragmentation patterns [24]. In the recent decade, chromatography is rarely used to detect glucose for practical and experimental purposes because relatively complex and time-consuming, requiring skilled technicians to operate and interpret results, often expensive, and requiring specialized equipment, reagents, and consumables [25].

Then, mass spectrometry involves separating and detecting glucose molecules based on their mass-to-charge ratio. The study by Rui et al. doing facile detection of glucose using mass spectrometry. The glucose is tested in the rat brain, and the mass spectrometry type is MALDI [26]. A study by Lyndsay et al. also used mass spectrometry coupled with gas chromatography. In addition, the glucose location targeted is the liver and skeletal muscle [27]. Meanwhile, the study reported by Andre et al. is focused on glucose metabolism in the different regions of the brain using imaging mass spectrometry because dysregulation increases the risk for depression and Alzheimer's disease [28]. However, mass spectrometry is a highly sensitive and specific technique for detecting and quantifying molecules. It has several disadvantages for glucose detection, such as complicated and time-consuming sample preparation process, instrumentation, and maintenance can be expensive and generate complex spectra that require expert interpretations [29].

In the electrochemical method, an electrode measures the current or voltage produced when glucose is oxidized or reduced at the electrode surface. Raquel et al. created a conductive filament modified with nickel nanoparticles to detect glucose, with a detection limit is 2.4 $\mu\text{mol/L}$ [30]. Rafiq et al. reported a study to detect glucose based on electrochemical non-enzymatic using CuO nanoleaves, with a detection limit of 12 nM [31]. They also produce the metal oxide, especially NiO, in the nanosheet to detect glucose, and the detection limit improved to 2.5 μM [32]. Meanwhile, Hyosang et al. use

porous-induced graphene as an electrode, with a detection limit of under 300 nM [33]. Then, Qingpeng et al. also produced a device integrated with paper-based microfluidic to detect glucose, with a detection limit of 5 μM [34]. This method has some drawbacks, i.e., it can be interfered with by other electroactive specimens in the sample, require frequent calibration, not be sensitive enough to detect low glucose levels, and require extensive sample preparations [35]. The extended overview of glucose detection using nanoparticles based on the electrochemical method is shown in Table 2.

Table 2 - The overview of the glucose detection method using nanoparticles based on the electrochemical platform

Year	Author [ref]	Sample	Nanoparticle	Structure	Detection limit (μM)	Detail of analytical characteristics
2013	Kuo-Chiang <i>et al.</i> [36]	0 – 8 mM	Ni/Cu/CNT	Composite	0.25	The linear ranges obtained in two areas, i.e., $2.5 \times 10^{-8} - 2 \times 10^{-4}$ M and $2 \times 10^{-3} - 8 \times 10^3$ M, with the sensitivity value, is $2633 \mu\text{Acm}^2\text{mM}^{-1}$ and $2,437 \mu\text{Acm}^2\text{mM}^{-1}$, respectively.
2014	Jingwei <i>et al.</i> [37]	0 – 6 mmol/L	Ni-MoS ₂	Sheet	0.31	The sensitivity is obtained in $1,824 \mu\text{Acm}^2\text{mM}^{-1}$, with the R ² value is 0.9971. The linearity is conducted up to 4 mM. In addition, the RSD value is 3.7 %.
2015	Jing <i>et al.</i> [38]	0.5 μM – 23 mM	CuO-C	Spherical	0.1	The sensitivity is $2,981 \mu\text{Acm}^2\text{mM}^{-1}$, with the value of signal-to-noise-ratio being 3. Then, the RSD value is 3.48 %.
2016	Mehdi <i>et al.</i> [39]	1 nM – 350 μM	Ag-C	Composite	0.0003	Time response is 4 s, with R ² value is 0.9976. Also, RSD value is 5.2 %.
2018	Mohapatra <i>et al.</i> [40]	0.09 – 28 mM	C	Onion	90	The sensitivity is achieved in $26.5 \mu\text{Acm}^2\text{mM}^{-1}$, with a linear response in 1 – 10 mM.
2019	Mahmoud <i>et al.</i> [41]	0.001 – 100 μM	Cu-ZnO	Spherical	0.001	The sensitivity is $0.06 \mu\text{Acm}^2\text{mM}^{-1}$, and the highest error value through samples is 7.92 μM. Meanwhile, the lowest error value is 3.4 μM.
2019	Asif <i>et al.</i> [42]	0 – 100 μM	NiO	Thin film	1	The sensitivity is $49.9 \mu\text{Acm}^2\text{mM}^{-1}$, with a regression value is 0.997. Then, the linear response is obtained in concentrations 0.1 μM – 8 mM. Then, the time detection needed is less than 12 s.
2020	Raquel <i>et al.</i> [30]	75 – 1,000 μmol/L	Ni	Spherical	55.6	The RSD value is < 5 %, the R ² value is 0.999, and the sensitivity is $0.095 \mu\text{A}\mu\text{mol}^{-1}\text{L}$.
2020	Rafiq <i>et al.</i> [32]	0.25 – 3.75 mM	NiO	Sheet	2.5	The sensor sensitivity is $1,618.4 \mu\text{AmM}^{-1}\text{cm}^{-2}$. The minimal buffer solution needed is 100 – 150 μL; the required potential is +0.37 V. The R ² value is 0.9975.
2020	Hyosang <i>et al.</i> [33]	0 – 160 mg/dL	Graphene	Porous	0.3	The sensitivity is $4.622 \mu\text{A}/\text{mM}$, with an R ² value is 0.99. The error value is 0.36 – 0.66 μA.
2020	Pinak <i>et al.</i> [43]	5 μM – 0.225 mM	CuO	Porous	0.41	The sensitivity is $3072 \mu\text{AmM}^{-1}\text{cm}^{-2}$, with a coefficient regression is 0.998.
2021	Rafiq <i>et al.</i> [31]	0.005 – 5.89 mM	CuO	Leave	0.012	The sensitivity is obtained in $1467.32 \mu\text{A}/(\text{mMcm}^2)$, with an RSD value of 3.4 %.
2022	Artur <i>et al.</i> [44]	0.2 – 2.4 mM	Fe ₃ O ₄ @PNE-GOx	Spherical	6.1	The device can be used for 20 weeks non-stop, with a sensitivity of $97.34 \mu\text{AmM}^{-1}\text{cm}^{-2}$. Then, the time response is 8 s.
2022	Kubilay <i>et al.</i> [45]	0.05 μM – 1.6 mM	NiCo@MWCNT	Composite	0.26	The sensitivity is $10,015 \mu\text{AmM}^{-1}\text{cm}^{-2}$, with the R ² value is 0.9284.

4. Localized Surface Plasmon Resonance

This section is divided into two parts, i.e., the theory of the Localized Surface Plasmon Resonance and plasmonic sensor. The theory of the Localized Surface Plasmon Resonance is discussed in Section 4.1, which focuses on the general expression and equation used. For the plasmonic sensor, it is discussed in Section 4.2, which focuses on the specific equation used for plasmonic sensor analysis to detect certain analytes.

4.1 Theory of Localized Surface Plasmon Resonance

Localized Surface Plasmon Resonance (LSPR) is the collaborative fluctuation of electrons associated with the electric field on the metal / dielectric surface, as shown in Fig. 2. The resulting spectral position depends on the substance's shape, size, and composition related to the refractive index on the metal/dielectric surface. The process of shifting the absorbance spectrum is based on changes in the refractive index value of the surrounding medium so that biomolecular interactions occur on the surface of the nanostructures. Referring to Mie's theory [46], the optical phenomenon of LSPR strongly refers to the geometry of the metal nanostructures. Different fabrication methods to produce specific nanostructures can produce different LSPR phenomena effects, both increasing and decreasing [47].

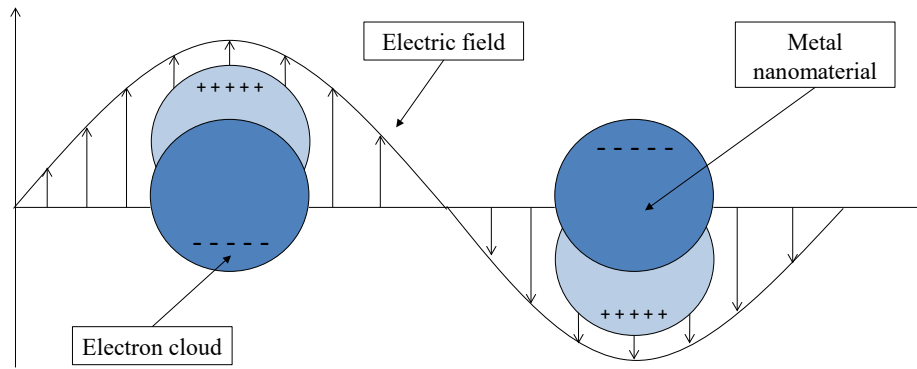


Fig. 2 – LSPR phenomenon in collective electrons excitation [47]

When a series of multipolar oscillations on a metal nanospherical is determined by its boundary conditions, the extinction cross-section (C_{ext}) value is obtained as Equation (1) [48].

$$C_{ext} = \frac{2\pi V}{3\lambda} \varepsilon_m^{3/2} \sum_j \frac{(1 + P_j^2) \varepsilon_i}{\left(\varepsilon_r + \left(1 - \frac{P_j}{P_j}\right) \varepsilon_m \right)^2 + \varepsilon_i^2} \quad (1)$$

where,

- V : volume of particles used
- λ : wavelength
- ε_m : dielectric constant of the surrounding medium
- ε_i : dielectric constant of the particle in the imaginer number
- ε_r : dielectric constant of the particle in the real number
- P_j : depolarization factor

The value of the depolarization factor for the elongated particle is discussed as follows:

$$P_{length} = \frac{1 - e^2}{e^2} \left[\frac{1}{2e} \ln \left(\frac{1 + e}{1 - e} \right) - 1 \right] \quad (2)$$

$$P_{width} = \frac{1 - P_{length}}{2} \quad (3)$$

where e is defined as ellipticity and given by:

$$e^2 = 1 - \left(\frac{\text{length}}{\text{width}}\right)^{-2} \tag{4}$$

Thus, particles with an ellipsoidal shape have strong spectra polarization-dependent, where a small change in aspect ratio causes a significant change in the extinction band. When the nanoparticle has a size of 10 - 100 nm, the resulting LSPR spectrum will shift toward red with a shift of around 47 nm [49].

4.2 Plasmonic Sensor

A plasmonic sensor is a sensor that utilizes the LSPR phenomenon produced by noble metal nanoparticles such as gold [50], silver [51], and platinum [52] to detect various types of analytes. Although silver has more sensitivity than silver, gold has the advantage of chemical stability and resistance to oxidation [46]. In addition, the LSPR produced by gold is within the visible range so that it can be observed and analyzed using UV-Vis spectroscopy. Other advantages possessed by gold as a sensing material include having an outer electron configuration in the d shell so that it is inert and does not quickly react to other substances in the environment. Furthermore, gold also has good conductivity, good catalytic activity, and is non-toxic [53].

When analytes interact with the surface of the gold nanoparticle, the refractive index on the surface of the nanoparticle changes, causing a shift in the peak of the LSPR spectrum. The modification and shape of the nanoparticle also influence the changing frequency of the LSPR spectral peaks. Nanoparticles with asymmetric shapes have a high sensitivity to changes in surface bonding compared to spherical shapes. Changes in the LSPR frequency, when the binding process occurs are represented in Equation (5). This value allows for the unique sensitivity of noble nanoparticles to detect the presence of biological molecular binding on the surface [54]. The illustration of LSPR response in binding analytes is represented in Fig. 3.

$$\Delta\lambda = m(\Delta n) \left[1 - \exp\left(\frac{-2d}{l_d}\right)\right] \tag{5}$$

where,

- m : refractive index sensitivity
- Δn : refractive index shift
- d : effective adsorbate layer thickness
- l_d : electromagnetic field decay length

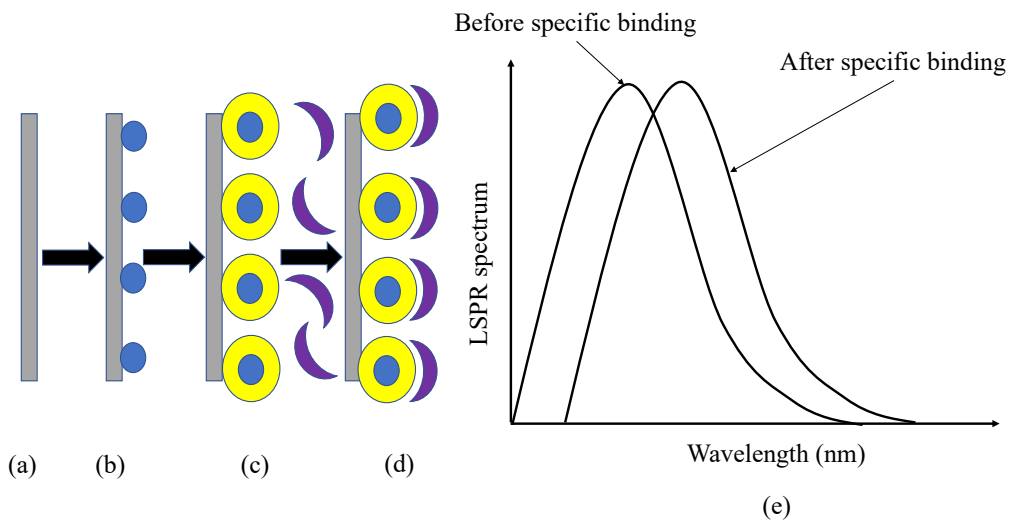


Fig. 3 - LSPR response for sensor application from (a) choose substrate; (b) attachment of metal nanoparticles; (c) modification of metal nanoparticles; (d) attachment of analyte on metal nanoparticles changed the spectrum LSPR shift as shown in (e) [47]

The refractive index sensitivity is linear to changes in wavelength. Thus, the refractive index sensitivity is defined as the shift in wavelength per refractive index unit (nm/RIU), as shown in Equation (6) [55].

$$m = \frac{\Delta\lambda}{\Delta n} \tag{6}$$

where,

$\Delta\lambda$: LSPR peak shift

Δn : refractive index shift

Although the change in refractive index is proportional to the change in wavelength, the ability to detect small changes depends on the resulting spectrum's sharpness, which is usually quantified by its full-width half maximum (FWHM). To obtain this value, it is necessary to calculate the figure of merit as described in Equation (7) [56].

$$FOM = \frac{m}{FWHM} \tag{7}$$

Then, the plasmonic sensors usually use components of light absorption, luminescence, fluorescence, Raman scattering, reflectance, and refractive index [57]. The detection method is based on material sensing, but transmission and reflection are popular and widely applied methods for analyte detection. This mode comprises a light source, fiber optic, chamber to place substrate/analyte, spectrometer/detector, and computer. Previous studies about formaldehyde detection using gold nanoparticles [58], boric acid detection using gold nanoplates [59], and glyphosate detection using gold nanobipyramids [60], are using this configuration with modification in the chamber. The schematic setup of this detection mode is shown in Fig. 4.

Conversely, the absorption mode is also promising for analyte detection. This configuration consists of a similar instrument to the previous configuration but differs in setup style because of different fiber optics. For example, in herbicide detection using gold nanorods, an absorption method also consists of a light source, fiber optic, chamber, spectrometer, and computer to analyze the spectrum absorbance [61]. The schematic setup is shown in Fig. 5.

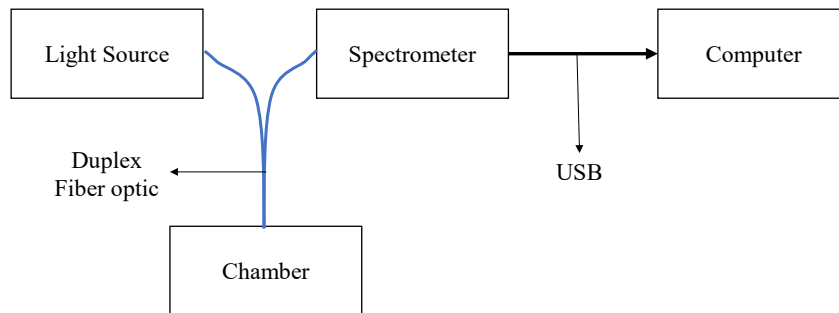


Fig. 4 - Schematic setup of reflection mode

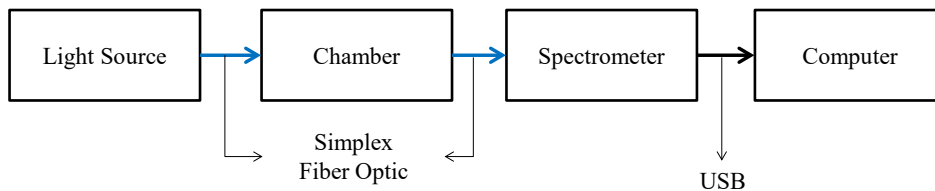


Fig. 5 - Schematic setup of the plasmonic sensor using the absorption method

Then, the plasmonic sensor can be classified as label-free or label-based, depending on whether or not a label or a biomolecule is attached to the sensing surface. In a label-free LSPR sensor, the sensing surface is typically functionalized with a receptor molecule such as an antibody, aptamer or DNA strand, which can selectively capture the target analyte without needing a label [62]. When the target analyte binds to the receptor, it induces a change in the refractive index of the sensing layer and leads to a shift in the LSPR wavelength, which can be measured by the instrument [63]. Label-free LSPR sensors are attractive for their simplicity, high sensitivity, and ability to detect real-time binding events without additional chemical reagents. In contrast, label-based LSPR sensors use a label or a biomolecule conjugated to a nanoparticle to amplify the LSPR signal. For example, in GNPs-based LSPR sensors, the nanoparticle acts as a plasmonic label that enhances the sensor's sensitivity by providing an additional LSPR signal that can be detected. The label can be functionalized with a receptor molecule binding to the target analyte. Label-based LSPR sensors can offer higher

sensitivity than label-free sensors but require additional steps to prepare the labeled particles and are less versatile in their applications [64].

Glucose detection is also can obtain using plasmonic sensors. These methods use glucose or glucose-related molecules' light absorption or emission properties to detect glucose concentration. The phenomenon used LSPR and attracted the researchers to gain more invention and innovation using several nanoparticles with various shapes and modifications. For example, Hyeong-min *et al.* used the LSPR phenomenon to detect glucose by utilizing GNPs functionalized with amine@POSS-aminophenylboronic acid as material sensing [65]. Another research uses SiO₂ with a 1050 nm/RIU sensitivity by Anis *et al.* [66]. Dennyson *et al.* also utilized the LSPR phenomenon but used Bi₂Se₃, which is synthesized by the microwave-assisted method. This sensor has a limit of detection of 6.1 μM [67]. Then, research by Hamid investigated that ring shape air@Agcore@shell nanoparticles are sensitive to surrounding medium change, with the figure of merit value being 14.53 [68]. The continued overview of glucose detection based on the LSPR phenomenon is shown in Table 3.

Table 3 – The overview of the plasmonic sensor for glucose detection

Year	Author [ref]	Sample	Nanoparticle	Structure	Detection limit (μM)	Detail of analytical characteristics
2012	Sachin <i>et al.</i> [69]	0 – 13900 μM	Au	Spherical	1.4	Using a U-shaped probe with a bending radius of 0.982 mm.
2013	Xin <i>et al.</i> [70]	0 – 500 mM	Au	Rods	0.1	The R ² value is 0.990, with oxidation recorded in 0.25 mM. The analytes used for selectivity tests are ascorbic acid, dopamine, and uric acid.
2015	Dachao <i>et al.</i> [71]	1 – 1000 mg/dL	Borate polymer PAA-ran-PAAPBA	Layer	55.59	The resolution at 12 polymer layers is 1 mg/dL with an R ² value of 0.998.
2015	Jitendra <i>et al.</i> [72]	1 ng/mL – 6 μg/mL	Au	Hollow	0.005	RIS value to be found in 47.3 ± 2.9 ΔI/RIU with the R ² value is 0.99. The linear response is obtained in 1.33 – 1.36 RIU.
2015	Martin <i>et al.</i> [73]	0 – 100 mM	Au	Antenna	50	The noise level as low as 0.1 nm with the extrapolation of 2.5 and 1 mM glucose relates to 0.05 mM. Also, the shift for this range is 0.1 nm.
2017	Hsueh <i>et al.</i> [74]	0 – 20 mg/dL	Au	Spherical	55.59	The sensing material with 20 nm size produces a sensitivity of 8.1 nm/mM with the linearity denoted by an R ² value of 0.985
2018	Yu-Sheng <i>et al.</i> [75]	0 – 20 %	SiO ₂ -Au	Thin film	-	The sensor's sensitivity is 157.61 nm/RIU with an FOM of 5.25. The stable bandwidth reaches 30 nm, with the shift of the resonant obtained at 56 nm.
2018	Huizhen <i>et al.</i> [76]	0.01 – 30 mM	Au/AET-PMBA	Spherical	0.08	The R ² value is 0.9938, and the resonant wavelength shifts are 16.5 nm. As a comparison, for lactose, the resonant wavelength shift is 18.45 nm.
2020	Dennyson [67]	10 – 100 μM	Bi ₂ Se ₃	Layer	6.1	The sensitivity is 0.112 μAμM ⁻¹ with losses obtained in 17 % after 19 days of non-stop use.
2020	Hamie <i>et al.</i> [68]	0 – 10 mM	Ag	Spherical	1000	The figure of merit is 14.53, with an FWHM value of 61.3 nm yields.
2020	Qingshan <i>et al.</i> [77]	0 – 11 mM	Au-GO	Fiber	2,260	The sensor's sensitivity is 1.06 nm/mM with an autocorrelation accuracy of 0.9386.
2021	Hyeong <i>et al.</i> [65]	1 – 1 M	Au	Spherical	25	The coefficient of variation is 9.28 %, with an R ² value is 0.996.

2022	Junxi <i>et al.</i> [78]	1 nM – 5 mM	AuNPs/Ex-TFG	Spherical	0.0025	Peak change in redshift at several wavelengths, i.e., 0.24 nm, 0.06 nm, and 0.48 nm. The 3 regions of linear response are 1 nM – 1 μ M, 1 μ M – 50 μ M, and 50 μ M – 5 mM.
2022	Lingqiao <i>et al.</i> [79]	0.3 – 0.4 mol/L	Ag/Au	Spherical	300,000	The maximum sensitivity is 1144.07407 nm/RIU.
2022	Junjie <i>et al.</i> [80]	0 – 1 mM	Au/Ag	Core shell	-	The linearity is obtained by an R ² value of 0.9799.
2023	Jiaming <i>et al.</i> [81]	0 – 300 mg/dL	Cr/Au/Graphene	Thin film	55.59	The sensor's sensitivity is 1813.89 nm/RIU, which is 2.1 times higher than without graphene.

5. Summary and Future Prospective

Glucose becomes an important indicator in diabetes to stay within the normal range. The conventional methods for glucose detection are glucose meters and urine testing, which have several drawbacks to be improved. Advanced methods have been developed and act as alternative glucose detection methods, such as chromatographic, mass spectrometry, electrochemical, and plasmonic sensor. Plasmonic sensors that utilize the optical phenomenon LSPR have promising performance in detecting glucose due to their advantage, i.e., non-invasive, real-time monitoring, and to be sensitive surrounding medium change. Plasmonic sensors can produce different analytical characteristics using various nanoparticles as sensing materials. This condition causes the plasmonic sensor to be an alternative method that attracts interest in innovation and invention.

Acknowledgment

This work is supported by Universiti Tun Hussein Onn Malaysia (UTHM) through Tier 1 (vot H916). The authors would like to thank Microelectronics and Nanotechnology – Shamsuddin Research Centre, Universiti Tun Hussein Onn Malaysia for the laboratory facilities.

References

- [1] J. Yang, R. Zhou, and Z. Ma, "Autophagy and energy metabolism," *Autophagy Biol. Dis. Basic Sci.*, pp. 329–357, 2019, doi: 10.1007/978-981-15-0602-4_16.
- [2] P. Manza *et al.*, "Brain network segregation and glucose energy utilization: relevance for age-related differences in cognitive function," *Cereb. Cortex*, vol. 30, no. 11, pp. 5930–5942, 2020, doi: 10.1093/cercor/bhaa167.
- [3] Q. Lu *et al.*, "The role of long noncoding RNA in lipid, cholesterol, and glucose metabolism and treatment of obesity syndrome," *Med. Res. Rev.*, vol. 41, no. 3, pp. 1751–1774, 2021, doi: 10.1002/med.21775.
- [4] S. Demir, P. P. Nawroth, S. Herzig, and B. Ekim Üstünel, "Emerging targets in type 2 diabetes and diabetic complications," *Adv. Sci.*, vol. 8, no. 18, p. 2100275, 2021, doi: 10.1002/adv.202100275.
- [5] J. Balaban, R. Bijelic, S. Milicevic, K. Stanetic, and N. Grbic, "Correlation between extracutaneous microvascular complications and diabetic foot ulcers in patients with type 2 diabetes mellitus," *Med. Arch.*, vol. 74, no. 6, p. 444, 2020, doi: 10.5455%2Fmedarh.2020.74.443-448.
- [6] D. Kibirige *et al.*, "Indicators of optimal diabetes care and burden of diabetes complications in Africa: a systematic review and meta-analysis," *BMJ Open*, vol. 12, no. 11, p. e060786, 2022, doi: 10.1136/bmjopen-2022-060786.
- [7] R. Ganguly, S. V. Singh, K. Jaiswal, R. Kumar, and A. K. Pandey, "Modulatory effect of caffeic acid in alleviating diabetes and associated complications," *World J. Diabetes*, vol. 14, no. 2, p. 62, 2023, doi: 10.4239%2Fwj.d.v14.i2.62.
- [8] L. Tang, S. J. Chang, C. J. Chen, and J. T. Liu, "Non-invasive blood glucose monitoring technology: A review," *Sensors (Switzerland)*, vol. 20, no. 23, pp. 1–32, 2020, doi: 10.3390/s20236925.
- [9] S. Jang, Y. Wang, and A. Jang, "Review of emerging approaches utilizing alternative physiological human body fluids in non-or minimally invasive glucose monitoring," in *Advanced Bioscience and Biosystems for Detection and Management of Diabetes*, Springer, 2022, pp. 9–26. doi: 10.1007/978-3-030-99728-1_2.
- [10] J. Guo, B. Zhou, Z. Du, C. Yang, L. Kong, and L. Xu, "Soft and plasmonic hydrogel optical probe for glucose monitoring," *Nanophotonics*, vol. 10, no. 13, pp. 3549–3558, 2021, doi: 10.1515/nanoph-2021-0360.
- [11] E. Ujah, M. Lai, and G. Slaughter, "Ultrasensitive tapered optical fiber refractive index glucose sensor," *Sci. Rep.*, vol. 13, no. 1, p. 4495, 2023, doi: 10.1038/s41598-023-31127-4.
- [12] H. Chehregosha, M. E. Khamseh, M. Malek, F. Hosseinpanah, and F. Ismail-Beigi, "A view beyond HbA1c: role of continuous glucose monitoring," *Diabetes Ther.*, vol. 10, pp. 853–863, 2019, doi: 10.1007/s13300-019-0619-1.
- [13] R. Balaji, R. Duraisamy, and M. P. Kumar, "Complications of diabetes mellitus: A review," *Drug Invent. Today*, vol. 12, no. 1, 2019.

- [14] R. E. Sand, "Nomenclature and structure of carbohydrate hydrocolloids," in *Food Hydrocolloids*, CRC Press, 2020, pp. 19–46.
- [15] S. Liu, W. Su, and X. Ding, "A review on microfluidic paper-based analytical devices for glucose detection," *Sensors (Switzerland)*, vol. 16, no. 12, pp. 1–17, 2016, doi: 10.3390/s16122086.
- [16] I. G. U. Pascal, J. N. Ofoedu, N. P. Uchenna, A. A. Nkwa, and G.-U. E. Uchamma, "Blood glucose control and medication adherence among adult type 2 diabetic Nigerians attending a primary care clinic in under-resourced environment of eastern Nigeria," *N. Am. J. Med. Sci.*, vol. 4, no. 7, p. 310, 2012, doi: 10.4103/2F1947-2714.98590.
- [17] J. A. Bluestone, J. H. Buckner, and K. C. Herold, "Immunotherapy: Building a bridge to a cure for type 1 diabetes," *Science (80-)*, vol. 373, no. 6554, pp. 510–516, 2021, doi: 10.1126/science.abh1654.
- [18] A. Berbudi, N. Rahmadika, A. I. Tjahjadi, and R. Ruslami, "Type 2 diabetes and its impact on the immune system," *Curr. Diabetes Rev.*, vol. 16, no. 5, pp. 442–449, 2020, doi: 10.2174/1573399815666191024085838.
- [19] A. Fujishima, Y. Onodera, H. Miura, and Y. Terada, "Anti-glutamic acid decarboxylase antibody-positive gestational diabetes mellitus with autoimmune type 1 diabetes mellitus in the early postpartum period: A case report and literature review," *Tohoku J. Exp. Med.*, vol. 259, no. 4, pp. 327–333, 2023, doi: 10.1620/tjem.2023.J013.
- [20] H.-W. Huang *et al.*, "An automated all-in-one system for carbohydrate tracking, glucose monitoring, and insulin delivery," *J. Control. Release*, vol. 343, pp. 31–42, 2022, doi: <https://doi.org/10.1016/j.jconrel.2022.01.001>.
- [21] X. Luo, J. Xia, X. Jiang, M. Yang, and S. Liu, "Cellulose-based strips designed based on a sensitive enzyme colorimetric assay for the low concentration of glucose detection," *Anal. Chem.*, vol. 91, no. 24, pp. 15461–15468, Dec. 2019, doi: 10.1021/acs.analchem.9b03180.
- [22] S. Balbach *et al.*, "Smartphone-based colorimetric detection system for portable health tracking," *Anal. Methods*, vol. 13, no. 38, pp. 4361–4369, 2021, doi: 10.1039/d1ay01209f.
- [23] W.-Q. Xie, Y.-X. Gong, and K.-X. Yu, "Rapid quantitative detection of glucose content in glucose injection by reaction headspace gas chromatography," *J. Chromatogr. A*, vol. 1520, pp. 143–146, 2017, doi: <https://doi.org/10.1016/j.chroma.2017.09.018>.
- [24] P. N. Wahjudi, M. E. Patterson, S. Lim, J. K. Yee, C. S. Mao, and W.-N. P. Lee, "Measurement of glucose and fructose in clinical samples using gas chromatography/mass spectrometry," *Clin. Biochem.*, vol. 43, no. 1, pp. 198–207, 2010, doi: <https://doi.org/10.1016/j.clinbiochem.2009.08.028>.
- [25] L. E. Fitri, T. Widaningrum, A. T. Endharti, M. H. Prabowo, N. Winaris, and R. Y. B. Nugraha, "Malaria diagnostic update: From conventional to advanced method," *J. Clin. Lab. Anal.*, vol. 36, no. 4, pp. 1–14, 2022, doi: 10.1002/jcla.24314.
- [26] R. Chen *et al.*, "High-salt-tolerance matrix for facile detection of glucose in rat brain microdialysates by MALDI mass spectrometry," *Anal. Chem.*, vol. 84, no. 1, pp. 465–469, Jan. 2012, doi: 10.1021/ac202438a.
- [27] L. E. A. Young *et al.*, "Accurate and sensitive quantitation of glucose and glucose phosphates derived from storage carbohydrates by mass spectrometry," *Carbohydr. Polym.*, vol. 230, p. 115651, 2020, doi: <https://doi.org/10.1016/j.carbpol.2019.115651>.
- [28] A. Kleinriders *et al.*, "Regional differences in brain glucose metabolism determined by imaging mass spectrometry," *Mol. Metab.*, vol. 12, pp. 113–121, 2018, doi: <https://doi.org/10.1016/j.molmet.2018.03.013>.
- [29] A. J. Grooms, B. J. Burris, and A. K. Badu-Tawiah, "Mass spectrometry for metabolomics analysis: Applications in neonatal and cancer screening," *Mass Spectrom. Rev.*, vol. n/a, no. n/a, p. e21826, Dec. 2022, doi: <https://doi.org/10.1002/mas.21826>.
- [30] R. G. Rocha *et al.*, "Production of 3D-printed disposable electrochemical sensors for glucose detection using a conductive filament modified with nickel microparticles," *Anal. Chim. Acta*, vol. 1132, pp. 1–9, 2020, doi: <https://doi.org/10.1016/j.aca.2020.07.028>.
- [31] R. Ahmad *et al.*, "Engineered hierarchical CuO nanoleaves based electrochemical nonenzymatic biosensor for glucose detection," *J. Electrochem. Soc.*, vol. 168, no. 1, p. 017501, 2021, doi: 10.1149/1945-7111/abd515.
- [32] R. Ahmad, M. Khan, N. Tripathy, M. I. R. Khan, and A. Khosla, "Hydrothermally synthesized nickel oxide nanosheets for non-enzymatic electrochemical glucose detection," *J. Electrochem. Soc.*, vol. 167, no. 10, p. 107504, 2020, doi: 10.1149/1945-7111/ab9757.
- [33] H. Yoon *et al.*, "A chemically modified laser-induced porous graphene based flexible and ultrasensitive electrochemical biosensor for sweat glucose detection," *Sensors Actuators B Chem.*, vol. 311, p. 127866, 2020, doi: <https://doi.org/10.1016/j.snb.2020.127866>.
- [34] Q. Cao, B. Liang, T. Tu, J. Wei, L. Fang, and X. Ye, "Three-dimensional paper-based microfluidic electrochemical integrated devices (3D-PMED) for wearable electrochemical glucose detection," *RSC Adv.*, vol. 9, no. 10, pp. 5674–5681, 2019, doi: 10.1039/c8ra09157a.
- [35] H. Huang *et al.*, "Electrochemical monitoring of persistent toxic substances using metal oxide and its composite nanomaterials: Design, preparation, and application," *TrAC Trends Anal. Chem.*, vol. 119, p. 115636, 2019, doi: 10.1016/j.trac.2019.115636.
- [36] K.-C. Lin, Y.-C. Lin, and S.-M. Chen, "A highly sensitive nonenzymatic glucose sensor based on multi-walled carbon nanotubes decorated with nickel and copper nanoparticles," *Electrochim. Acta*, vol. 96, pp. 164–172, 2013, doi: <https://doi.org/10.1016/j.electacta.2013.02.098>.

- [37] J. Huang, Y. He, J. Jin, Y. Li, Z. Dong, and R. Li, "A novel glucose sensor based on MoS₂ nanosheet functionalized with Ni nanoparticles," *Electrochim. Acta*, vol. 136, pp. 41–46, 2014, doi: <https://doi.org/10.1016/j.electacta.2014.05.070>.
- [38] J. Zhang, J. Ma, S. Zhang, W. Wang, and Z. Chen, "A highly sensitive nonenzymatic glucose sensor based on CuO nanoparticles decorated carbon spheres," *Sensors Actuators B Chem.*, vol. 211, pp. 385–391, 2015, doi: <https://doi.org/10.1016/j.snb.2015.01.100>.
- [39] M. Baghayeri, A. Amiri, and S. Farhadi, "Development of non-enzymatic glucose sensor based on efficient loading Ag nanoparticles on functionalized carbon nanotubes," *Sensors Actuators B Chem.*, vol. 225, pp. 354–362, 2016, doi: <https://doi.org/10.1016/j.snb.2015.11.003>.
- [40] J. Mohapatra *et al.*, "Enzymatic and non-enzymatic electrochemical glucose sensor based on carbon nano-onions," *Appl. Surf. Sci.*, vol. 442, pp. 332–341, 2018, doi: [10.1016/j.apsusc.2018.02.124](https://doi.org/10.1016/j.apsusc.2018.02.124).
- [41] A. Mahmoud, M. Echabaane, K. Omri, L. El Mir, and R. Ben Chaabane, "Development of an impedimetric non enzymatic sensor based on ZnO and Cu doped ZnO nanoparticles for the detection of glucose," *J. Alloys Compd.*, vol. 786, pp. 960–968, 2019, doi: <https://doi.org/10.1016/j.jallcom.2019.02.060>.
- [42] A. Hayat *et al.*, "Nickel oxide nano-particles on 3D nickel foam substrate as a non-enzymatic glucose sensor," *J. Electrochem. Soc.*, vol. 166, no. 15, p. B1602, 2019, doi: [10.1149/2.0491915jes](https://doi.org/10.1149/2.0491915jes).
- [43] P. Chakraborty, S. Dhar, N. Deka, K. Debnath, and S. P. Mondal, "Non-enzymatic salivary glucose detection using porous CuO nanostructures," *Sensors Actuators B Chem.*, vol. 302, p. 127134, 2020, doi: <https://doi.org/10.1016/j.snb.2019.127134>.
- [44] A. Jędrzak, M. Kuznowicz, T. Rębiś, and T. Jesionowski, "Portable glucose biosensor based on polynorepinephrine@magnetite nanomaterial integrated with a smartphone analyzer for point-of-care application," *Bioelectrochemistry*, vol. 145, p. 108071, 2022, doi: <https://doi.org/10.1016/j.bioelechem.2022.108071>.
- [45] K. Arikan, H. Burhan, R. Bayat, and F. Sen, "Glucose nano biosensor with non-enzymatic excellent sensitivity prepared with nickel-cobalt nanocomposites on f-MWCNT," *Chemosphere*, vol. 291, p. 132720, 2022, doi: <https://doi.org/10.1016/j.chemosphere.2021.132720>.
- [46] K. M. Mayer and J. H. Hafner, "Localized surface plasmon resonance sensors," *Chem. Rev.*, vol. 111, no. 6, pp. 3828–3857, 2011, doi: [10.1021/cr100313v](https://doi.org/10.1021/cr100313v).
- [47] K. Khurana and N. Jaggi, "Localized surface plasmonic properties of Au and Ag nanoparticles for sensors: A review," *Plasmonics*, vol. 16, no. 4, pp. 981–999, 2021, doi: [10.1007/s11468-021-01381-1](https://doi.org/10.1007/s11468-021-01381-1).
- [48] M. Hu *et al.*, "Gold nanostructures: Engineering their plasmonic properties for biomedical applications," *Chem. Soc. Rev.*, vol. 35, no. 11, pp. 1084–1094, 2006, doi: [10.1039/b517615h](https://doi.org/10.1039/b517615h).
- [49] L. M. Liz-Marzán, "Tailoring surface plasmons through the morphology and assembly of metal nanoparticles," *Langmuir*, vol. 22, no. 1, pp. 32–41, 2006, doi: [10.1021/la0513353](https://doi.org/10.1021/la0513353).
- [50] F. Yaghubi, M. Zeinoddini, A. R. Saeedinia, A. Azizi, and A. Samimi Nemati, "Design of localized surface plasmon resonance (LSPR) biosensor for immunodiagnostic of E. coli O157: H7 using gold nanoparticles conjugated to the chicken antibody," *Plasmonics*, vol. 15, pp. 1481–1487, 2020, doi: [10.1007/s11468-020-01162-2](https://doi.org/10.1007/s11468-020-01162-2).
- [51] A. Taghavi, F. Rahbarizadeh, S. Abbasian, and A. Moshaii, "Label-free LSPR prostate-specific antigen immunosensor based on GLAD-fabricated silver nano-columns," *Plasmonics*, vol. 15, pp. 753–760, 2020, doi: [10.1007/s11468-019-01049-x](https://doi.org/10.1007/s11468-019-01049-x).
- [52] I. Antohe, I. Iordache, V.-A. Antohe, and G. Socol, "A polyaniline/platinum coated fiber optic surface plasmon resonance sensor for picomolar detection of 4-nitrophenol," *Sci. Rep.*, vol. 11, no. 1, p. 10086, 2021, doi: [10.1038/s41598-021-89396-w](https://doi.org/10.1038/s41598-021-89396-w).
- [53] N. Momeni, K. Javadifar, M. A. Patrick, M. H. Hasan, and F. Chowdhury, "A review on gold nanoparticles-based biosensors in clinical and non-clinical applications," *Int. J. Eng. Mater. Manuf.*, vol. 7, no. 1, pp. 1–12, 2022, doi: [10.26776/ijemm.07.01.2022.01](https://doi.org/10.26776/ijemm.07.01.2022.01).
- [54] S. Unser, I. Bruzas, J. He, and L. Sagle, "Localized surface plasmon resonance biosensing: Current challenges and approaches," *Sensors (Switzerland)*, vol. 15, no. 7, pp. 15684–15716, 2015, doi: [10.3390/s150715684](https://doi.org/10.3390/s150715684).
- [55] Y. Xu *et al.*, "Optical refractive index sensors with plasmonic and photonic structures: promising and inconvenient truth," *Adv. Opt. Mater.*, vol. 7, no. 9, p. 1801433, 2019, doi: [10.1002/adom.201801433](https://doi.org/10.1002/adom.201801433).
- [56] B. Doiron *et al.*, "Quantifying figures of merit for localized surface plasmon resonance applications: a materials survey," *Acs Photonics*, vol. 6, no. 2, pp. 240–259, 2019, doi: [10.1021/acsp Photonics.8b01369](https://doi.org/10.1021/acsp Photonics.8b01369).
- [57] Y. Jeong, Y. M. Kook, K. Lee, and W. G. Koh, "Metal enhanced fluorescence (MEF) for biosensors: General approaches and a review of recent developments," *Biosens. Bioelectron.*, vol. 111, no. January, pp. 102–116, 2018, doi: [10.1016/j.bios.2018.04.007](https://doi.org/10.1016/j.bios.2018.04.007).
- [58] M. H. Jali *et al.*, "Formaldehyde sensor with enhanced performance using microsphere resonator-coupled ZnO nanorods coated glass," *Opt. Laser Technol.*, vol. 139, no. December 2020, 2021, doi: [10.1016/j.optlastec.2020.106853](https://doi.org/10.1016/j.optlastec.2020.106853).
- [59] M. Morsin, M. M. Salleh, A. A. Umar, and M. Z. Sahdan, "Gold nanoplates for a localized surface plasmon resonance-based boric acid sensor," *Sensors (Switzerland)*, vol. 17, no. 5, pp. 1–9, 2017, doi: [10.3390/s17050947](https://doi.org/10.3390/s17050947).
- [60] S. Nafisah *et al.*, "Improved sensitivity and selectivity of direct localized surface plasmon resonance sensor using

- gold nanobipyramids for glyphosate detection,” *IEEE Sens. J.*, vol. 20, no. 5, pp. 2378–2389, 2020, doi: 10.1109/JSEN.2019.2953928.
- [61] N. Z. An’Nisa, M. Morsin, R. Sanudin, N. L. Razali, and S. Nafisah, “Controlled wet chemical synthesis of gold nanorods for triclopyr butotyl herbicide detection based-plasmonic sensor,” *Sens. Bio-Sensing Res.*, vol. 29, p. 100359, 2020, doi: 10.1016/j.sbsr.2020.100359.
- [62] B. I. Karawdeniya *et al.*, “Surface functionalization and texturing of optical metasurfaces for sensing applications,” *Chem. Rev.*, vol. 122, no. 19, pp. 14990–15030, 2022, doi: 10.1021/acs.chemrev.1c00990.
- [63] E. Mauriz and L. M. Lechuga, “Plasmonic biosensors for single-molecule biomedical analysis,” *Biosensors*, vol. 11, no. 4, p. 123, 2021, doi: 10.3390/bios11040123.
- [64] C. S. Huertas, O. Calvo-Lozano, A. Mitchell, and L. M. Lechuga, “Advanced evanescent-wave optical biosensors for the detection of nucleic acids: An analytic perspective,” *Front. Chem.*, vol. 7, p. 724, 2019, doi: 10.3389/fchem.2019.00724.
- [65] H. M. Kim, W. J. Kim, K. O. Kim, J. H. Park, and S. K. Lee, “Performance improvement of a glucose sensor based on fiber optic localized surface plasmon resonance and anti-aggregation of the non-enzymatic receptor,” *J. Alloys Compd.*, vol. 884, p. 161140, 2021, doi: 10.1016/j.jallcom.2021.161140.
- [66] A. Omidniaee, S. Karimi, and A. Farmani, “Surface plasmon resonance-based SiO₂ kretschmann configuration biosensor for the detection of blood glucose,” *Silicon*, vol. 14, no. 6, pp. 3081–3090, 2022, doi: 10.1007/s12633-021-01081-9.
- [67] A. D. Savariraj *et al.*, “Microwave-assisted synthesis of localized surface plasmon resonance enhanced bismuth selenide (Bi₂Se₃) layers for non-enzymatic glucose sensing,” *J. Electroanal. Chem.*, vol. 856, p. 113629, 2020, doi: <https://doi.org/10.1016/j.jelechem.2019.113629>.
- [68] H. Heidarzadeh, “Highly sensitive plasmonic sensor based on ring shape nanoparticles for the detection of ethanol and d-glucose concentration,” *IEEE Trans. Nanotechnol.*, vol. 19, pp. 397–404, 2020, doi: 10.1109/TNANO.2020.2993907.
- [69] S. K. Srivastava, V. Arora, S. Sapra, and B. D. Gupta, “Localized surface plasmon resonance-based fiber optic U-shaped biosensor for the detection of blood glucose,” *Plasmonics*, vol. 7, no. 2, pp. 261–268, 2012, doi: 10.1007/s11468-011-9302-8.
- [70] X. Liu *et al.*, “A plasmonic blood glucose monitor based on enzymatic etching of gold nanorods,” *Chem. Commun.*, vol. 49, no. 18, pp. 1856–1858, 2013, doi: : 10.1039/c3cc38476d.
- [71] D. Li *et al.*, “Glucose affinity measurement by surface plasmon resonance with borate polymer binding,” *Sensors Actuators A Phys.*, vol. 222, pp. 58–66, 2015, doi: 10.1016/j.sna.2014.10.039.
- [72] J. Satija, J. Tharion, and S. Mukherji, “Facile synthesis of size and wavelength tunable hollow gold nanostructures for the development of a LSPR based label-free fiber-optic biosensor,” *RSC Adv.*, vol. 5, no. 86, pp. 69970–69979, 2015.
- [73] M. Mesch, C. Zhang, P. V Braun, and H. Giessen, “Functionalized hydrogel on plasmonic nanoantennas for non-invasive glucose sensing,” *Acs Photonics*, vol. 2, no. 4, pp. 475–480, 2015, doi: 10.1021/acsphotonics.5b00004.
- [74] H.-T. Chou, W.-H. Huang, T.-M. Wu, Y.-K. Yu, and H.-C. Hsu, “LSPR based glucose sensor using au nanoparticles fabricated by photochemical method,” in *2017 International Conference on Applied System Innovation (ICASI)*, 2017, pp. 1591–1594. doi: 10.1109/ICASI.2017.7988235.
- [75] Y.-S. Lin and W. Chen, “A large-area, wide-incident-angle, and polarization-independent plasmonic color filter for glucose sensing,” *Opt. Mater. (Amst.)*, vol. 75, pp. 739–743, 2018, doi: 10.1016/j.optmat.2017.11.043.
- [76] H. Yuan *et al.*, “Fiber-optic surface plasmon resonance glucose sensor enhanced with phenylboronic acid modified Au nanoparticles,” *Biosens. Bioelectron.*, vol. 117, pp. 637–643, 2018, doi: 10.1016/j.bios.2018.06.042.
- [77] Q. Yang *et al.*, “Highly sensitive and selective sensor probe using glucose oxidase/gold nanoparticles/graphene oxide functionalized tapered optical fiber structure for detection of glucose,” *Optik (Stuttg.)*, vol. 208, p. 164536, 2020, doi: 10.1016/j.ijleo.2020.164536.
- [78] J. Zhang *et al.*, “Ultrasensitive glucose biosensor using micro-nano interface of tilted fiber grating coupled with biofunctionalized au nanoparticles,” *IEEE Sens. J.*, vol. 22, no. 5, pp. 4122–4134, 2022, doi: 10.1109/JSEN.2022.3144203.
- [79] L. Li, W. Cui, Z. He, W. Xue, and H. He, “Plasmonic sensor based on silver nanoparticles for the detection of glucose,” *Plasmonics*, vol. 17, no. 3, pp. 1231–1234, 2022, doi: 10.21203/rs.3.rs-1121070/v1.
- [80] J. Wang *et al.*, “Plasmonic Sensing of Glucose Based on Gold–Silver Core–Shell Nanoparticles,” *Chemosensors*, vol. 10, no. 10, p. 404, 2022, doi: 10.3390/chemosensors10100404.
- [81] J. Ma, B. Lu, P. Zhang, D. Li, and K. Xu, “Liquid transfer of graphene to the cylindrical gold nanostructures for sensitivity enhancements of SPR glucose sensor,” *Sensors Actuators A Phys.*, vol. 353, p. 114227, 2023, doi: 10.1016/j.sna.2023.114227.